Free Radical Biology and Medicine 229 (2025) 213–224

Contents lists available at ScienceDirect

Free Radical Biology and Medicine

journal homepage: www.elsevier.com/locate/freeradbiomed

Characterizing oxidative stress induced by Aβ oligomers and the protective role of carnosine in primary mixed glia cultures

Vincenzo Cardaci [a], Lucia Di Pietro [b,c], Matthew C. Zupan [d], Jay Sibbitts [d,e], Anna Privitera [b,f], Susan M. Lunte [d,e,g], Filippo Caraci [b,h], Meredith D. Hartley [d,**], Giuseppe Caruso [b,h,*]

[a] Università Vita-Salute San Raffaele, Milano, Italy
[b] Department of Drug and Health Sciences, University of Catania, Catania, Italy
[c] Scuola Superiore di Catania, University of Catania, Catania, Italy
[d] Department of Chemistry, University of Kansas, Lawrence, KS, USA
[e] Ralph N. Adams Institute for Bioanalytical Chemistry, University of Kansas, Lawrence, KS, USA
[f] Department of Biomedical and Biotechnological Sciences, University of Catania, Catania, Italy
[g] Department of Pharmaceutical Chemistry, University of Kansas, Lawrence, KS, USA
[h] Unit of Neuropharmacology and Translational Neurosciences, Oasi Research Institute-IRCCS, Troina, Italy

ARTICLE INFO

Keywords:
Reactive oxygen species
Neurodegeneration
Alzheimer's disease
Oxidative stress
Carnosine
Microglia
Astrocytes

ABSTRACT

Alzheimer's disease (AD) is a neurodegenerative disorder characterized by cognitive decline and memory loss. A critical aspect of AD pathology is represented by oxidative stress, which significantly contributes to neuronal damage and death. Microglia and astrocytes, the primary glial cells in the brain, are crucial for managing oxidative stress and supporting neuronal function. Carnosine is an endogenous dipeptide possessing a multimodal mechanism of action that includes antioxidant, anti-inflammatory, and anti-aggregant activities. The present study investigated the effects of Aβ1-42 oligomers (oAβ), small aggregates associated with the neurodegeneration observed in AD, on primary rat mixed glia cultures composed of both microglia and astrocytes, focusing on the ability of these detrimental species to induce oxidative stress. We assessed intracellular reactive oxygen species (ROS) and nitric oxide (NO) levels as markers of oxidative stress. Exposure to oAβ significantly elevated both ROS and NO intracellular levels compared to control cells. However, this effect was completely inhibited by the pre-treatment of mixed cultures with carnosine, resulting in ROS and NO levels similar to those observed in untreated (control) cells. Single-cell analysis of cellular responses to oAβ revealed heterogeneous ROS production, resulting in two distinct clusters of cells, one of which was very responsive to the treatment. The presence of carnosine counteracted the overproduction of ROS, also leading to a single, homogeneous cluster, similar to that observed in the case of control cells. Interestingly, unlike ROS response, single-cell analysis of NO production did not show any distinct clusters. Overall, our findings demonstrated the ability of carnosine to mitigate Aβ-induced oxidative stress in mixed glia cells, by rescuing ROS and NO intracellular levels, as well as to normalize the heterogeneous response to the treatment measured in terms of clusters' formation. The present study suggests a therapeutic potential of carnosine in pathologies characterized by oxidative stress including AD.

1. Introduction

Alzheimer's disease (AD) is the most common neurodegenerative disorder worldwide, characterized by progressive cognitive decline, memory impairment, and behavioral changes [1]. The pathophysiology underlying AD is complex, multifactorial, and not yet entirely elucidated.

It is well-known that amyloid-β (Aβ), one of the peptides implicated in AD pathogenesis, can aggregate, starting from soluble monomers and progressing to higher molecular weight species including oligomers, protofibrils, and mature fibrils [2]. While Aβ monomers appear to have physiological brain functions [2], mounting evidence suggests a pivotal role for Aβ oligomers (oAβ) in initiating and perpetuating neuronal injury and dysfunction [3]. oAβ exhibit neurotoxicity, disrupt synaptic

* Corresponding author. Department of Drug and Health Sciences, University of Catania, Viale Andrea Doria, 6, Catania, 95125, Italy.
** Corresponding author. Department of Chemistry, University of Kansas, 2030 Becker Drive, Lawrence, KS, 66047, USA.
E-mail addresses: hartley@ku.edu (M.D. Hartley), giuseppe.caruso2@unict.it (G. Caruso).

https://doi.org/10.1016/j.freeradbiomed.2025.01.030
Received 7 September 2024; Received in revised form 18 December 2024; Accepted 13 January 2025
Available online 16 January 2025

function, promote oxidative stress, and trigger neuroinflammation, all of which contribute to the progressive neurodegeneration observed in the brain of AD patients [4–6].

Oxidative stress, characterized by an imbalance between the production of reactive oxygen (ROS) and nitrogen (RNS) species and the antioxidant defense mechanisms, has emerged as a prominent feature in the pathogenesis of AD [7], but the intricate interplay between AD and oxidative stress is still not well understood [8,9]. Moreover, oxidative stress has emerged as a key player in promoting the oligomerization of Aβ peptides, activating β- and γ-secretase enzymes, fundamental in the generation of various Aβ species, thereby crucially contributing to the accumulation of toxic aggregates [10,11].

Compelling evidence from both animal models and clinical studies underscores the pervasive influence of oxidative stress in AD pathophysiology [12,13]. Notably, oxidative stress markers have been detected in AD animal models prior to plaque deposition, suggesting their involvement in the early stages of disease development. Furthermore, the presence of oxidative stress markers in the brains, plasma, and erythrocytes of individuals with mild cognitive impairment (MCI) and AD underlines the relevance of this process in the disease continuum [12,14]. In this context, identifying strategies to mitigate oAβ-induced oxidative stress could represent a promising therapeutic approach in AD.

Microglia and astrocytes, the primary glial cell types in the central nervous system (CNS), play critical roles in the brain's response to injury and disease, including AD [15–17]. Astrocytes, the most abundant glial cells, are crucial for supporting neuronal function through a variety of mechanisms including the regulation of neurotransmitter balance, the metabolic support to neurons, and the maintenance of the integrity of the blood-brain barrier [18,19]. In response to injury or disease, astrocytes can become reactive [20,21]. Microglia, the resident immune cells of the brain, are essential for innate immune responses within the CNS and can rapidly change from a surveillant to an activated state upon detecting signals of damage or infection [22]. Microglia release pro-inflammatory cytokines, chemokines, and ROS in response to pathogens and facilitate immune reaction. However, chronic activation of microglia, as observed in neurodegenerative diseases like AD, can lead to sustained inflammation and neuronal damage [23].

The physiological interactions between astrocytes and microglia are critical for orchestrating a coordinated response to CNS insults [24]. Astrocytes can modulate microglial activity through the release of signaling molecules, which influence microglial activation states and functions [25]. In addition, microglia can affect astrocyte behavior by secreting factors that promote astrocytic reactivity and the release of neurotrophic or neurotoxic substances [26]. Both astrocytes and microglia aggregate around Aβ plaques and dystrophic neurites, contributing to the removal of these detrimental elements. However, their role in AD pathogenesis is too complex to determine due to the significant heterogeneity of these cells [27]. This heterogeneity includes molecular, morphological, and ultrastructural diversity, as well as their dynamic responsiveness and functions throughout the progression of AD [27] and may result in differential susceptibility to Aβ-induced damage among the different cell types [28,29]. The high variability in response to an injury, including Aβ-induced oxidative stress, makes the development of effective therapeutic strategies extremely difficult [30].

Carnosine is a naturally occurring dipeptide with a multimodal mechanism of action whose therapeutic potential has been considered for drug discovery processes in neurodegenerative disorders [31,32], pathological conditions often characterized by abnormal protein aggregation, oxidative stress, and inflammation, such as AD [33]. Carnosine has also shown the ability to mitigate the toxic responses of glial cells subjected to pro-oxidant and/or pro-inflammatory stimuli, including microglia [34] and astrocytes [35]. Furthermore, its ability to decrease oxidative stress and inflammation in different *in vitro* models of Aβ-induced inflammation [36,37], along with the capacity to modulate nitric oxide (NO) production and metabolism [38–40], make this molecule a promising candidate for drug discovery in AD.

Based on the above, we hypothesized that oAβ could exert a detrimental effect inducing oxidative stress through the production of ROS and/or RNS (i.e., NO) by glial cells, and that carnosine could counteract these phenomena.

In the present study, we first investigated the toxic potential of oAβ, used at 2 μM, a well-known concentration able to induce oxidative stress in different *in vitro* models [36,37,41,42], in primary rat mixed glia cultures, composed of astrocytes (~90%) and microglia (~10%). Additionally, to elucidate the molecular mechanisms underlying the toxic effects of oAβ, we studied the variation of the production of key elements related to oxidative/nitrosative stress, namely NO and total ROS. We also investigated the ability of carnosine to mitigate the production of reactive species induced by oAβ. Clustering analysis was employed to measure the heterogeneity of oAβ-induced reactive species production.

2. Materials and methods

2.1. Materials and reagents

The 1,1,1,3,3,3-hexafluoro-2-propanol (HFIP)-treated amyloid β-peptide (1-42) under the form of monomer was obtained from Bachem Distribution Services GmbH (Weil am Rhein, Germany). Fetal bovine serum (FBS), trypsin-EDTA solution consisting of 0.25% Trypsin/0.53 mM EDTA in Hank's Balanced Salt Solution (HBSS) without calcium or magnesium, and penicillin–streptomycin antibiotic solution (Pen/Strep) were all supplied by American Type Culture Collection (ATCC) (Manassas, VA, USA). Minimum Essential Medium (MEM), Dulbecco's Modified Eagle Medium (DMEM), L-Carnosine, MTT [3-(4,5-dimethylthiazol-2-yl)-2,5-diphenyltetrazolium bromide] tetrazolium salt, anhydrous dimethyl sulfoxide (DMSO), trypan blue solution, dulbecco's phosphate-buffered saline (DPBS), and phosphate-buffered saline (PBS) were obtained from Sigma Aldrich (St. Louis, MO, USA). The 4-amino-5-methylamino-2′,7′,-difluorofluorescein diacetate (DAF-FMDA), carboxyfluor escein (6-CF), and 2′,7′-dichlorodihydrofluorescein diacetate (H2DCF DA) probes, DMEM/Nutrient Mixture F-12 (DMEM/F12) (1:1) medium, GlutaMAX Supplement, 25 and 75 mL polystyrene culture flasks, 96-well plates, ethanol (95%), sodium hydroxide, boric acid, hydrochloric acid, CyQUANT™ LDH Cytotoxicity Assay kit, probenecid (water soluble), and C-Chip disposable hemocytometers were obtained from Thermo Fisher Scientific (Pittsburgh, PA, USA). One hundred fifty mL polystyrene culture flasks were supplied by Corning (Tewksbury, MA, USA). Centrifuge tubes equipped with 3 kDa molecular weight cut-off filters were purchased from VWR International (West Chester, PA, USA). The two reagents used for the preparation of the hybrid microfluidic devices, Sylgard 184 polydimethylsiloxane (PDMS) prepolymer and curing agent used in a 1:10 w/w ratio, were obtained from Ellsworth Adhesives (Germantown, WI, USA). Microglia Growth Supplement (MGS) was obtained from ScienCell Research Laboratories (Carlsbad, CA, USA). Pregnant Sprague Dawley rats at gestation day 13–16 were ordered from Charles River Laboratories (Stilwell, KS, USA). All water used was ultrapure (18.3 MΩ cm) (Milli-Q Synthesis A10, Millipore, Burlington, MA, USA).

2.2. Study approval

The use of primary mixed glia cultures obtained from neonatal rats was authorized by the Institutional Animal Care and Use Committee (IACUC) of the University of Kansas (#267-01).

2.3. Isolation and preparation of primary mixed glia cultures

Primary mixed glia cultures, pure astrocytes, and pure microglia were obtained from neonatal (P1-P2) rat cortices following a protocol previously described by Lian, Roy & Zheng, with slight modifications [43]. This protocol was used to isolate mixed glial cells, consisting of

astrocytes and microglia, as well as individual microglial and astroglial populations. The protocol consisted of two main steps: dissection of neonatal rat cortices and dissociation of glial cells.

In the first step, the neonatal rat pups were decapitated on a sterile gauze pad and their heads were rinsed with ice cold 70% ethanol. The cortical tissue was then dissected from the rest of the brain in a laminar flow cell culture hood and placed in a 50 mL conical tube containing HBSS on ice.

The cortical tissue was then dissociated as follows in the second step. The cortical tissue was triturated through a 25 mL pipette and then incubated with 0.125% trypsin at 37 °C for 15 min. The resulting cell suspension was then collected and 2 mL of FBS was added to quench the trypsin digestion. The trituration and trypsin digestion were repeated a second time on the remaining cortical tissue. The dissociated cells were then pooled, centrifuged, and the supernatant was carefully aspirated. Next, the cells were resuspended in growth medium, and the number of viable cells was counted. Then, about 1.2 million cells were seeded in a 150 mL polystyrene culture flask. The medium was changed after 4 days and then again after 7 days, and cells were collected after 11–12 days.

In order to determine the ratio of astrocytes/microglia, cells were separated and counted by using Countess 3 FL Automated Cell Counter (Thermo Fisher Scientific, Pittsburgh, PA, USA).

Mixed glial cells composed of astrocytes and microglia were used directly without further separation steps. Mixed glial cells grown in MEM supplemented with FBS (10%), GlutaMAX (1%), and Pen/Strep (1%), were plated on 25 mL polystyrene flasks or 96-well plates at a density of 2×10^4 cells/well.

Pure microglia were isolated from the mixed glial cell cultures by shaking the flasks, allowing the detachment of microglia, while astrocytes remained attached to the bottom of the flasks. The medium containing floating microglia was carefully aspirated, centrifuged, and the cells were then resuspended in complete medium consisting of DMEM supplemented with FBS (10%), GlutaMAX (1%), Pen/Strep (1%), and MGS (1%). The cells were then counted and plated in 96-well plates at a density of 2×10^4 cells/well.

The astrocytes attached on the bottom of the culture flasks were removed by trypsinization, resuspended in complete medium consisting of MEM supplemented with FBS (10%), GlutaMAX (1%), and Pen/Strep (1%). The cells were then counted and plated in 96-well plates at a density of 2×10^4 cells/well.

2.4. Cell culture and treatment

Primary mixed glia cultures, pure astrocytes, and pure microglia were treated with oAβ at a concentration of 2 μM for 24 h. The selection of the oAβ concentration was based on previous studies [36,37,41,42], showing its ability to achieve significant cell activation and response. In the case of primary mixed glia cultures, cells were pre-treated with carnosine (10 mM) for 1 h, a well-established protocol ensuring substantial uptake of carnosine before the exposure to stress-inducing agents [44]. This concentration of carnosine was already employed in previous *in vitro* studies with primary murine cells [42,36], ensuring maximal efficacy. At the end of the 24 h, for all the experimental conditions considered the number of viable cells was determined through the automated cell counter coupled to the use of a 0.4 % trypan blue solution.

2.5. oAβ preparation and treatment

The preparation of oAβ was achieved starting from lyophilized HFIP-treated Aβ1-42 monomers, following a protocol previously described in detail [45]. The HFIP-treated preparation was selected based on the well-known ability of HFIP to break down β-sheet structures, disrupt hydrophobic forces in aggregated amyloid preparations, and promote α-helical secondary structures. Briefly, the monomeric Aβ1-42 was first dissolved in DMSO, diluted in ice-cold DMEM/F12 (1:1) medium at the final concentration of 100 μM, and incubated at 4 °C under gentle rotation for 48 h to allow the formation of oAβ. At the end of the process, the oAβ were either immediately used to treat the different cell cultures or aliquoted and stored at −20 °C for future use.

2.6. Fluorescence assessment by ME-LIF and automated cell counter

The intracellular levels of ROS or NO in primary mixed glia cultures under our experimental conditions were determined by using both microchip electrophoresis with laser-induced fluorescence (ME-LIF) and an automated cell counter equipped with Invitrogen GFP EVOS LED Light Cubes. While the selection of the automated cell counter was based on its ability to measure the individual cell contributions, ME-LIF was selected to measure the fluorescence in the whole cell populations also ensuring to consider the real fluorescence due to the reaction between the probes (e.g., DAF-FMDA) and the molecules of interest (NO), then to discriminate our compounds from (if any) other fluorescent side products [36], something not feasible when using conventional immunofluorescence essays which do not allow electrophoretic separation of fluorescent products.

Two different compatible fluorescent probes, as per constructor declaration, were used. H2DCFDA was employed for the detection of ROS, while DAF-FMDA was used for the detection of NO. When performing ME-LIF, 6-CF was used as an internal standard [46].

Cells belonging to the different experimental conditions were harvested and an aliquot (100 μL) was used to assess the viability by using the automated cell counter coupled to the use of a 0.4% trypan blue solution. The remaining cells were centrifuged at 1100 rpm for 5 min, the supernatant was removed, and the pellet was resuspended in 200 μL of the labeling solution consisting of DPBS, the selected probe (H2DCFDA or DAF-FMDA at the final concentration of 100 μM), and probenecid (2.5 mM). Cells were then incubated for 30 min at 37 °C on a dry bath heating block. At the end of the incubation, the cells were diluted by adding 800 μL of pre-warmed DPBS (37 °C) and centrifuged at 1100 rpm for 5 min. Next, the supernatant was removed, and the pellet was resuspended in 1 mL of DPBS. An aliquot of cells was used for fluorescence measurement by using the automated cell counter, while the remaining cells were centrifuged at 1100 rpm for 5 min. Once the supernatant was removed, cells were lysed in 50 μL of chilled pure ethanol, and the lysate solution was then filtered by using a 3 kDa molecular weight cut-off filter (12000 rpm for 10 min). Finally, 15 μL of the filtered cell lysate was added to 135 μL of running buffer consisting of 10 mM sodium tetraborate (pH 9.2), 0.2% Tween20, and 6-CF (internal standard) at the final concentration of 70 nM (H2DCFDA experiments) or 7 nM (DAF-FMDA experiments), to account for run-to-run variability in electrophoresis. Twenty μL of this solution was analyzed by ME-LIF as recently described [36], with a slight modification regarding the separations that were performed in reverse polarity mode. The detailed procedure allowing the fabrication of the disposable hybrid PDMS-glass microchips with a simple-T geometry has been described previously [47–49].

2.7. MTT assay

Metabolic status in primary mixed glia cultures, pure astrocytes, and pure microglia was assessed using the well-known MTT assay [50,51]. After the treatment with oAβ (2 μM; 24 h), cells were incubated for 2 h, at 37 °C with the MTT solution at a final concentration of 0.5 mg/mL. At the end of incubation step, the MTT solution was removed, the formazan crystals were melted by using the DMSO, and the absorbance was measured at 569 nm through a microplate reader (SpectraMax M5, Molecular Devices, Sunnyvale, CA, USA). The values obtained were expressed as percent variation from the values detected in untreated cells representing the control.

2.8. LDH assay

The CyQUANT™ LDH Cytotoxicity Assay kit was used as a colorimetric assay to assess the toxicity induced by oAβ in primary mixed glia cultures, pure astrocytes, and pure microglia, in accordance with the manufacturer's recommendations. The values obtained were expressed as percent variation from the values detected in untreated cells representing the control.

2.9. Griess assay

The indirect measurement of NO released on the medium through the measurement of its primary and more stable end product nitrite was performed by the Griess assay [38]. At the end of the stimulation protocol, an equal volume of Griess reagent and supernatant taken from each well was mixed, and after 15 min at room temperature in the dark the absorbance was measured at 540 nm through a microplate reader (SpectraMax M5). The values obtained were expressed as percent variation from the values detected in untreated cells representing the control.

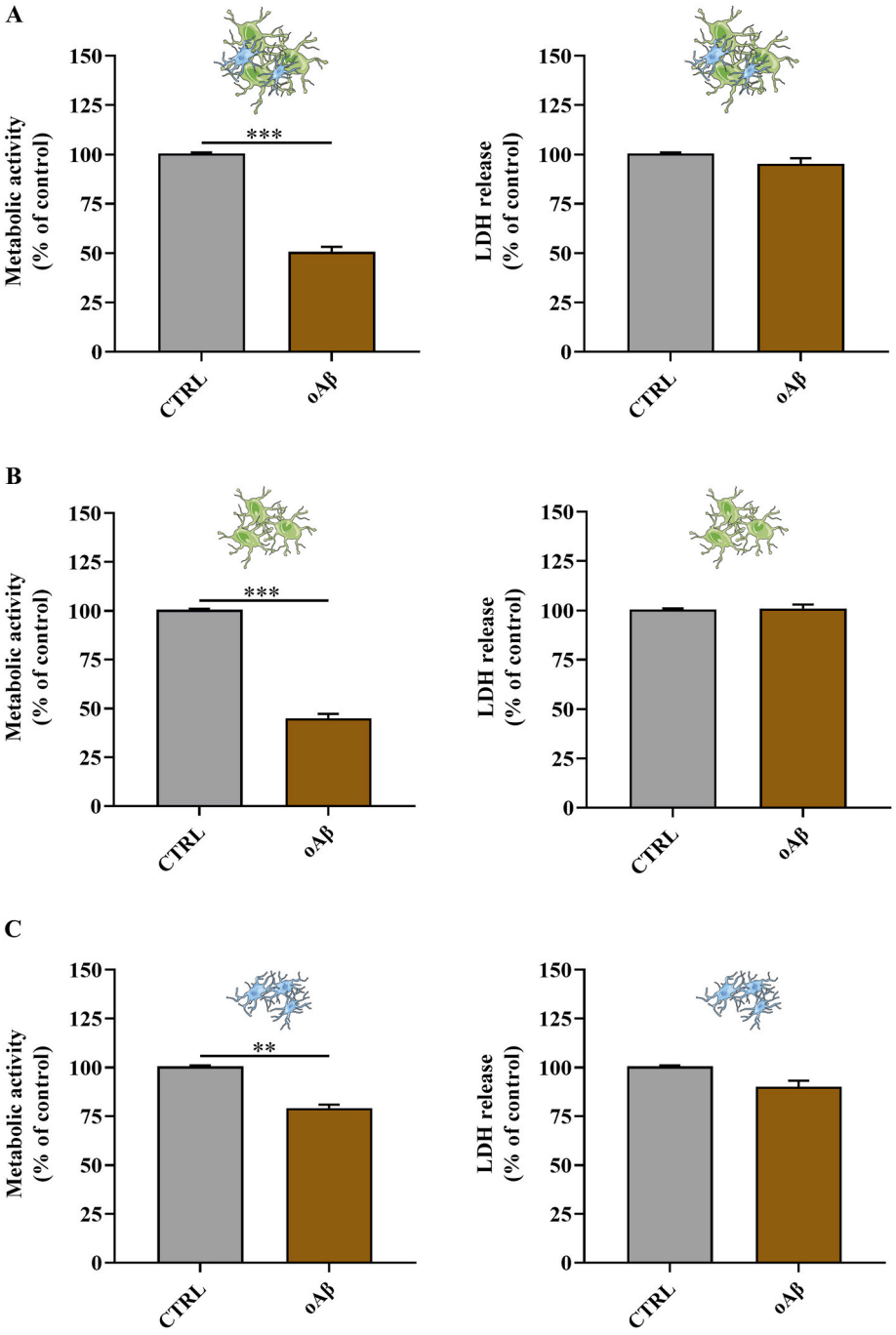

Fig. 1. Change in cell metabolic activity and LDH release caused by challenging primary mixed glia cultures and pure astrocytes or microglia with oAβ. (A) Mixed glia cultures, (B) pure astrocytes, or (C) pure microglia were treated for 24 h with oAβ (2 μM). Data are the mean of four samples and are expressed as the percent variation with respect to the cell metabolic activity or LDH release recorded in untreated (CTRL) cells. S.E.M. are represented by vertical bars. **Significantly different, $p < 0.01$; ***significantly different, $p < 0.001$.

2.10. Clustering analysis

The dataset included single-cell measurements from samples subjected to the different experimental conditions, encompassing three characteristics: cell size, circularity, and fluorescent intensity. The presence of batch effects was assessed through Principal Component Analysis (PCA), plotting the first two principal components of each batch. No evidence of batch effects was assessed. Prior to clustering analyses, preprocessing steps involving normalization using built-in MATLAB R2023b (The MathWorks Inc., Netick, Massachusetts USA) functions "normalize" and "zscore" were conducted. K-means clustering was performed using the “kmeans” function, with the optimal number of clusters determined via the gap statistic evaluation method facilitated by the "evalclusters’’ function.

2.11. Statistical analysis

Statistical analyses were conducted using GraphPad Prism 8.4.3 (GraphPad Software, Boston, Massachusetts USA). *t*-test was used when comparing two groups, while one-way analysis of variance (ANOVA) followed by Tukey’s *post hoc* was used for multiple comparison. Only two-tailed p-values less than 0.05 were considered statistically significant. All the experiments were performed at least in triplicate unless otherwise specified.

3. Results

3.1. oAβ decrease primary mixed glia cultures metabolic activity

The first aim of the present study was to investigate the changes in metabolic activity and cell toxicity occurring in primary mixed glia cultures as a consequence of oAβ used at 2 μM, a well-known concentration able to induce the production of ROS and NO in different *in vitro* models [36,37,41,42]. We also evaluated the possible individual (microglia or astrocytes) contribution to the observed effects. Fig. 1A shows a remarkable reduction in the metabolic activity of primary mixed glia cultures following the exposure to oAβ. When treating pure microglia or astrocytes, a more pronounced negative modulation of the metabolic activity was observed in astrocytes (Fig. 1B) compared to microglia (Fig. 1C). Interestingly, no significant differences between untreated (control) and oAβ-treated cells were observed when measuring the cell toxicity by performing the LDH assay (Fig. 1A–C).

In addition, the trypan blue exclusion test provided further proof that exposing mixed glial cells to oAβ did not cause cell toxicity (Fig. 2).

3.2. Carnosine prevents the increase in intracellular ROS and NO levels induced by oAβ in primary mixed glia cultures

Once the effects of oAβ on metabolic activity and cell toxicity of primary mixed glia cultures were determined, further experiments were conducted to assess the oxidative stress induced by oAβ, evaluated in terms of intracellular ROS levels, and to determine the ability of carnosine to counteract the pro-oxidant effects of oAβ.

As shown in Fig. 3A and B, oAβ induced a significant increase in the intracellular levels of ROS compared to that observed in control cells ($p < 0.001$). As clearly reported in the same figure, carnosine completely abolished the effects of oAβ, resulting in ROS intracellular levels similar to that observed in untreated cells.

Based on the results obtained by measuring ROS levels, the treatment of primary mixed glia cultures with oAβ also led to a significant increase in NO intracellular levels ($p < 0.05$) compared to untreated cells (Fig. 4A and B). Pre-treatment with carnosine significantly decreased intracellular NO levels, giving values even lower than that observed in untreated cells.

Interestingly, no differences were observed among the different experimental conditions when comparing the detectable levels of nitrite, the primary and more stable end product of NO, in the medium (Supplementary Fig. 1).

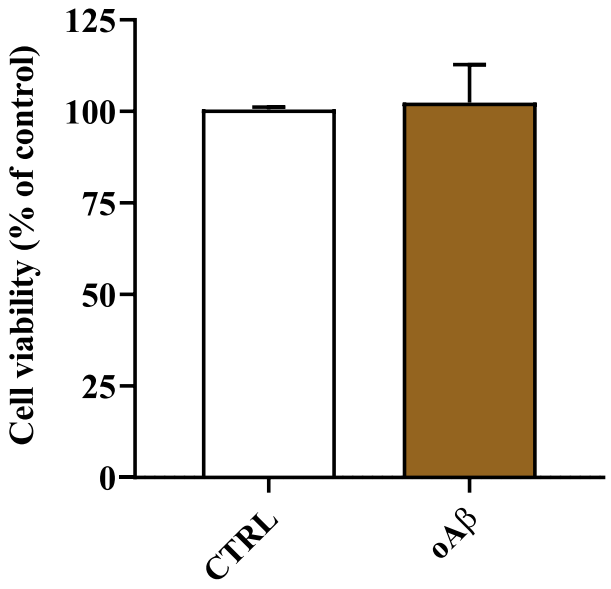

Fig. 2. Change in cell viability caused by challenging primary mixed glia cultures with oAβ. Cells were treated for 24 h with oAβ (2 μM). Data are the mean of four samples and expressed as the percent variation with respect to the ratio between live and dead cells recorded in untreated (CTRL) cells. S.E.M. are represented by vertical bars.

3.3. Carnosine normalizes the heterogeneous response of primary mixed glia cultures to oAβ measured in terms of ROS production

Fig. 5 reports 3D scatterplots depicting the multidimensional analysis of cellular responses to oAβ in the presence or absence of a carnosine pre-treatment. Each scatterplot represents a distinct experimental condition and displays normalized data along three dimensions: cell size, circularity, and fluorescence related to ROS production. In Fig. 5A, displaying untreated (control) cells, the application of clustering algorithms revealed a single predominant cluster. This suggests a homogeneous basal production of total ROS within the population of untreated cells. Interestingly, in the results reported in Fig. 5B, showing the response in oAβ-treated cells, the clustering algorithm identified two distinct clusters. Notably, these clusters were primarily segregated along the fluorescence dimension, indicating a heterogeneous production of ROS in response to the stimulation with oAβ. The ratio Cluster 1:Cluster 2, in term of number of cells, was calculated to be equal to 2.73:1, indicating a significant difference in their abundances. These findings suggest that only a subset of cells within the treated population was able to exhibit sustained ROS production in response to the exposure to oAβ. Fig. 5C depicts the data obtained from cells treated with oAβ in the presence of carnosine. Remarkably, the fluorescence distribution appears to be more compact compared to that observed in oAβ-treated cells and similar to that previously observed in untreated cells. It is also worth underlining that the clustering algorithm highlighted a single dominant cluster, as already observed in the case of untreated (control) cells. To further demonstrate that fluorescence intensity is the main contribution in the observed differences within the different experimental conditions, the data were plotted in terms of cell size and circularity (Fig. 5E). When analyzed without fluorescent intensity, there were no effects from Aβ or carnosine treatment.

In contrast to the intracellular ROS levels, analysis of NO did not

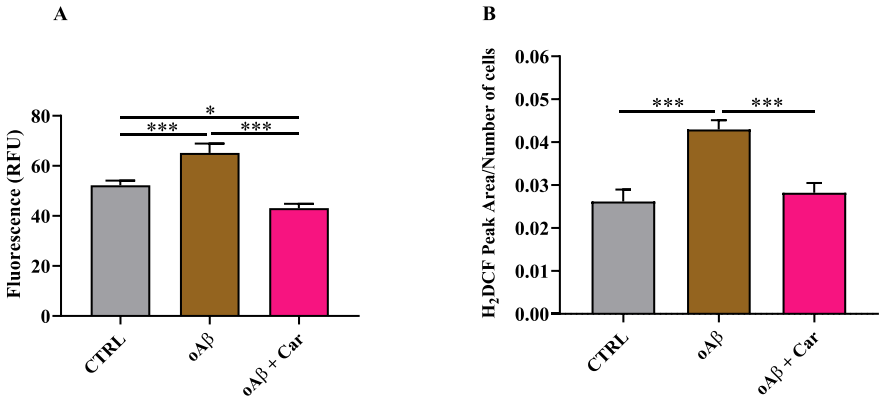

Fig. 3. Detection of intracellular concentrations of ROS. Fluorescence is expressed as (A) average Relative Fluorescence Unit (RFU) of H2DCF detected by automated cell counter or (B) average peak area corrected for number of cells detected by ME-LIF in resting mixed glia cells and in mixed glial cells treated 24 h with oAβ (2 μM), in the absence or presence of carnosine (Car) (10 mM, 1 h pre-treatment). For the ME-LIF data (B) signal intensity for H2DCF was normalized to 6-CF as an internal standard. Samples were compared by correcting the total signal for the total number of cells. A total of six runs/electropherograms for each sample were considered. Values are means ± S.E.M. of three to five samples. S.E.M. are represented by vertical bars. *Significantly different, $p < 0.05$; ***significantly different, $p < 0.001$.

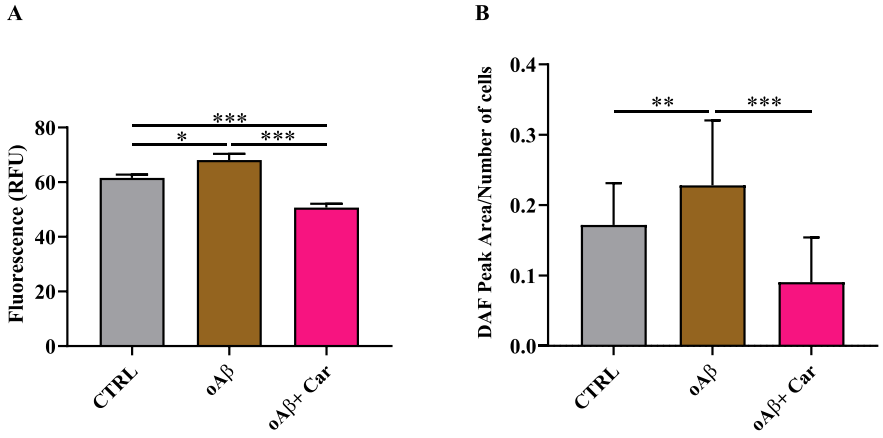

Fig. 4. Detection of intracellular concentrations of NO. Fluorescence is expressed as (A) average Relative Fluorescence Units (RFU) of DAF-FM detected by automated cell counter or (B) average peak area/number of cells detected by ME-LIF in resting mixed glia cells and in mixed glial cells treated 24 h with oAβ (2 μM), in the absence or presence of carnosine (Car) (10 mM, 1 h pre-treatment). Values are means ± S.E.M. of three samples. The ME-LIF data (B) was treated in the same manner as described in Fig. 3. A total of six runs/electropherograms for each sample were considered. S.E.M. are represented by vertical bars. *Significantly different, $p < 0.05$; **significantly different, $p < 0.01$; ***significantly different, $p < 0.001$.

reveal multiple clusters of cells (Fig. 6), suggesting a more uniform production due to oAβ exposure.

4. Discussion

Carnosine represents a naturally occurring endogenous molecule found in brain, innervated tissues, and the lens at concentrations up to 20 mM in humans [52], possessing a multimodal pharmacodynamic profile that includes its well-known direct and indirect antioxidant activity with the anti-inflammatory and anti-aggregant features at the CNS level [53–57], suggesting a potential therapeutic application for the treatment of diseases characterized by oxidative stress, neuroinflammation, and aberrant protein aggregation, such as AD [58]. Furthermore, as demonstrated by Fonteh et al. in a study measuring the free amino acid and dipeptide changes in the body fluids from healthy and probable AD (pAD) subjects, carnosine plasma levels are significantly reduced (∿50%) in pAD patients [59], suggesting that a deficit of this dipeptide is correlated with reduced global cognitive function.

Among the contributors to AD pathology, oAβ play a key role inducing oxidative stress that, at least in part, lead to neurodegenerative and neuroinflammatory phenomena as well as to impaired synaptic plasticity [37,60]. Different studies have shown the ability of oAβ to induce oxidative stress through multiple mechanisms [11,61], including impairment of mitochondrial function [13] and disruption of cellular redox homeostasis [62,63], also leading to the oxidative damage of lipids, proteins, and nucleic acids [64,65].

According to the above-described scenario, in the present study, we first explored the toxic potential of oAβ in primary mixed glia cultures, composed of astrocytes and microglia (9:1 ratio), measured in terms of metabolic activity and plasma membrane integrity. While no significant toxic effects were observed, there was a significant reduction in the metabolic activity of primary mixed glia cultures because of the exposure to oAβ compared to untreated (control) cells (Fig. 1A). The rational interpretation of the effects exerted by oAβ on glial cells was made possible by the application of a combination of "metabolic" (MTT assay) (Fig. 1) and "non-metabolic" (LDH assay and trypan blue exclusion test) (Figs. 1 and 2) methods [66], indicating that despite the lack of cell death, cells are suffering and the observed decrease of metabolic activity

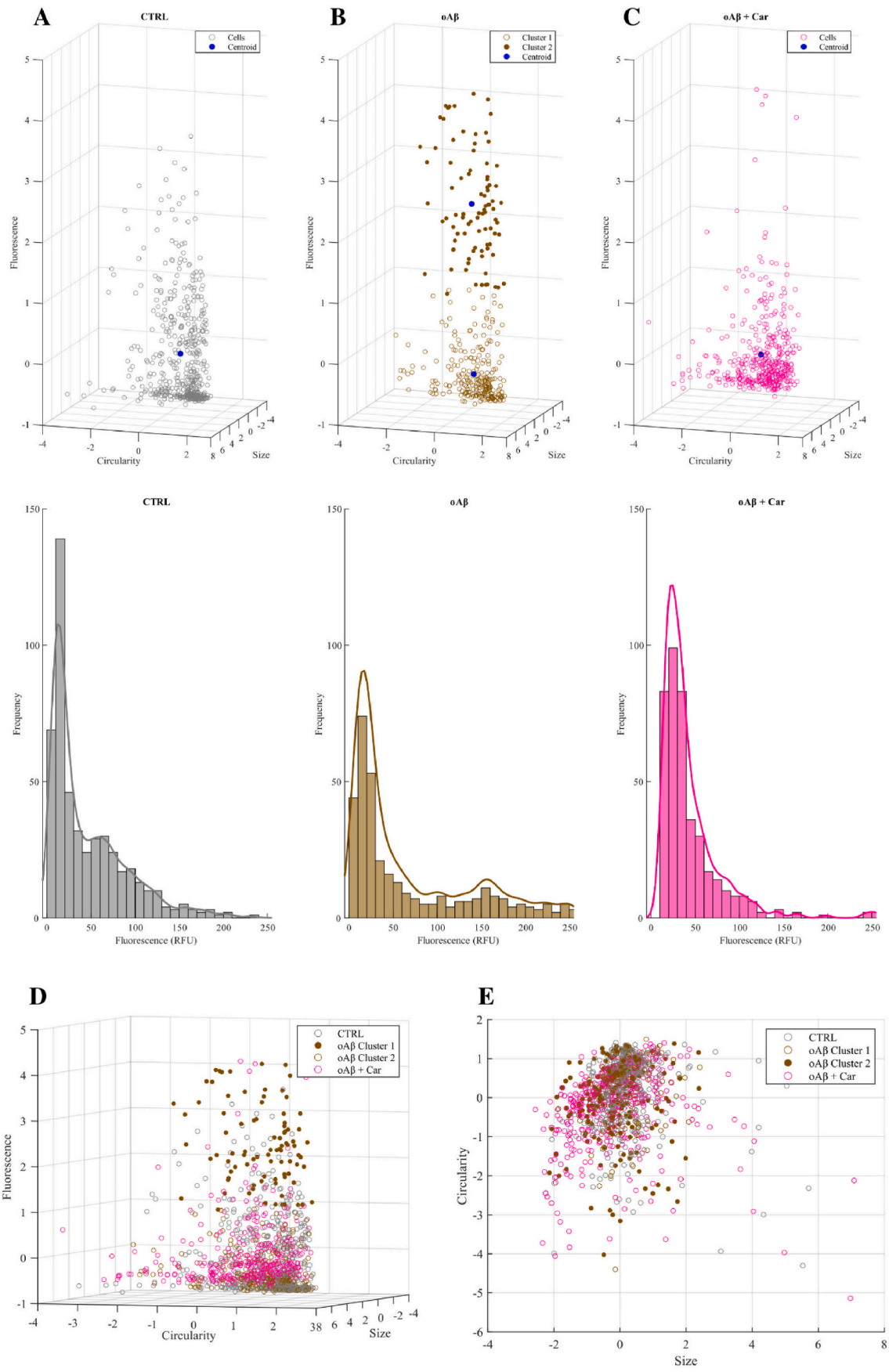

(caption on next page)

Fig. 5. 3D scatterplots and ROS fluorescence distributions of mixed glial cells. The 3D scatter plots depict size, circularity, and fluorescence of (A) untreated mixed glial cells, (B) mixed glial cells treated for 24 h with oAβ (2 μM), and (C) mixed glial cells treated for 24 h with oAβ in the presence of carnosine (Car) (10 mM, 1 h pre-treatment). Cytometry data were normalized using the z-score method. K-means optimal number of clusters, determined via the gap statistic evaluation method, is equal to two only in oAβ-treated cells (oAβ cluster 1 and oAβ cluster 2). Below each scatterplot is depicted the related fluorescence distribution. Each bin contains the cells in a 10 RFU gap. The overlaid line represents the kernel density estimation of the cells distribution. Fluorescence is expressed as Relative Fluorescence Units (RFU) of H2DCF. Mixed glial cells challenged with oAβ show a slight second peak around 150 RFU (B). Three samples of each experimental condition were analyzed. Results from the different experimental conditions are individually 3Dplotted and merged in (D). 2D scatter considering only size and circularity is shown in (E).

may be related to oxidative stress, in accordance to what was already demonstrated by Fresta et al. [39]. The observed differences in terms of metabolic activity between pure astrocytes and microglia may be attributable to the varying susceptibility of these cells to Aβ [67]. Our findings are also strongly in accordance with a study carried out by Kerokoski et al. showing that Aβ was able to significantly decrease the metabolic activity of neonatal rat astrocytes (decreased MTT reduction) in the absence of cell death, as underlined by the absence of changes in cellular ATP levels or lactate release [68]. Astrocytes are known to express high levels of Aβ receptors, rendering them particularly responsive to oAβ [69] and possibly mediating Aβ-induced neurotoxicity through inflammatory response [70]. It is also known that reactive astrocytes with high Aβ load are frequently found in the AD brain, further confirming the role of astrocytes in Aβ clearance [71]. Of note, astrocytes have shown a higher efficiency in uptaking Aβ compared to microglia, especially during the early stages of AD [72].

Once the effects of oAβ on metabolic activity and cell toxicity of glial cells were determined, additional experiments were devoted to assessing if the changes in metabolic activity were concomitant with oxidative stress, evaluated through the measurement of intracellular ROS and NO levels, two well-known mediators of the neurodegenerative phenomena observed in AD [73,74]. Based on the antioxidant and neuroprotective properties of carnosine, we also investigated its ability to counteract the well-known pro-oxidant effects of oAβ. In particular, carnosine was employed at a concentration of 10 mM, the same used by Distefano et al., employing primary mixed brain murine cultures [42] and Corona et al. [75], the latter showing the ability of carnosine to counteract molecular alterations and cognitive deficits in 3xTg-AD mice. Additionally, when used on human microglia, 10 mM carnosine was the highest non-toxic [76] concentration that maintained therapeutic efficacy [77]. Both ROS and NO intracellular levels were significantly increased following the exposure of primary mixed glia cultures to oAβ, while the presence of carnosine strongly inhibited the oAβ-induced changes, giving values comparable to that of control cells (Figs. 3 and 4). Our findings are in agreement with the ability of carnosine to directly interact with these pro-oxidant species [78], also as a consequence of the presence of histidine (imidazole ring) [38], in addition to numerous other studies in which carnosine counteracted oxidative stress in astrocytes and microglia [79] as well as in neuronal [80] and cerebellar [81] cells. Additional explanations of carnosine's antioxidant activity could depend on the enhanced uptake of the dipeptide in immune cells under pro-oxidant conditions [44], increasing the resilience of these cells to stress, as well as of the ability of carnosine to preserve the neuroprotective monomeric form of Aβ peptide or to disassemble the neurotoxic oAβ already formed [82,83]. Several additional activities exerted by carnosine on primary mixed cultures, indirectly supporting the observed antioxidant activity, could be represented by the modulation of TGF-β1 pathway [36] and the activation of insulin-degrading enzyme [42], an enzyme responsible for the degradation of both insulin and Aβ peptide. The ability of carnosine to regulate the intracellular levels of ROS and NO is of interest for several reasons. In fact, despite ROS serving as signaling molecules in various cellular processes [84], their dysregulation could lead to oxidative stress resulting in cellular dysfunction and contributing to the neurodegenerative processes observed in AD. Additionally, while low concentrations of NO contribute to normal neuronal communication and cerebral blood flow regulation, high levels can be neurotoxic, promoting oxidative stress and contributing to neurodegeneration [85]. Lastly, astrocytes and microglia are known to upregulate inducible nitric oxide synthase in response to inflammatory stimuli, leading to increased NO levels that can exacerbate Aβ pathology by enhancing inflammatory responses, also contributing to neuronal damage [85].

Since the single-cell analysis evidenced a heterogeneous production of ROS due to the challenge of mixed glial cells with oAβ, we lastly investigated the ability of carnosine to rescue the basal conditions.

While untreated (control) cells displayed a single predominant cluster, suggesting a homogeneous basal production of total ROS within this population (Fig. 5A), two distinct clusters were identified in the case of oAβ-treated cells (Fig. 5B), suggesting that only a subset of cells within the Aβ-treated population exhibited sustained ROS production. Single-cell analysis revealed that carnosine was able not only to rescue the basal intracellular levels of ROS, but also to abolish the heterogeneous response due to Aβ, leading to a single dominant cluster (Fig. 5C), as already observed in the case of untreated (control) cells. The above results, showing how the overall difference in terms of ROS levels is coming only from a responsive sub-population, highlight the importance of performing single-cell analysis. This analysis also demonstrated that the production of NO, was homogeneous, characterized by the absence of multiple clusters, suggesting a collective contribution from stimulated cells (Fig. 6). While previous studies have demonstrated carnosine's antioxidant properties in whole cell populations, our work is the first to reveal the heterogeneous nature of glial cell responses to Aβ-induced oxidative stress and carnosine's ability to normalize this response. This possibility is of great interest in the context of AD, widely known for its characteristic features, but for which the contribution of different brain cell types, even within the same population [86,87], is becoming increasingly important [88]. Our findings open new avenues for treatment that could slow or, in the best scenario, halt the progression of this disease. The lack of differences observed among the different experimental groups when comparing the extracellular release of NO could be due to the sub-toxic nature of the stimulation (i.e., oAβ), being able to trigger intracellular oxidative stress, without causing a significant damage of membrane integrity and cell death (Figs. 1A and 2), as previously observed in lung alveolar cells subjected to sub-toxic conditions [39]. With specific regards to carnosine's contribution, it is well-known that carnosine forms adducts with both NO and nitrite [38]; additionally, the decrease in NO could be due to a decreased synthesis [34], rather than degradation into its end product nitrite [40].

It is worth mentioning that our results were obtained by using a co-culture of astrocytes and microglia maintaining the *in vivo* architecture, something often obtained "artificially" by mixing two or more cells in a certain ratio and plating them on the same interface under specified conditions [89]. Maintaining the *status quo* is even more important when considering the interplay between astrocytes and microglia in AD [90] as well as their critical role in regulating oxidative stress and neuroinflammation [91], the understanding of which is critical for developing therapeutic strategies for diseases like AD. Finally, it is worth mentioning that our findings, obtained in primary cells, might differ in more complex *in vivo* systems; further *in vivo* studies, which provide the opportunity for a more accurate evaluation of the safety, toxicity, and efficacy, are needed to confirm this modulatory activity of carnosine.

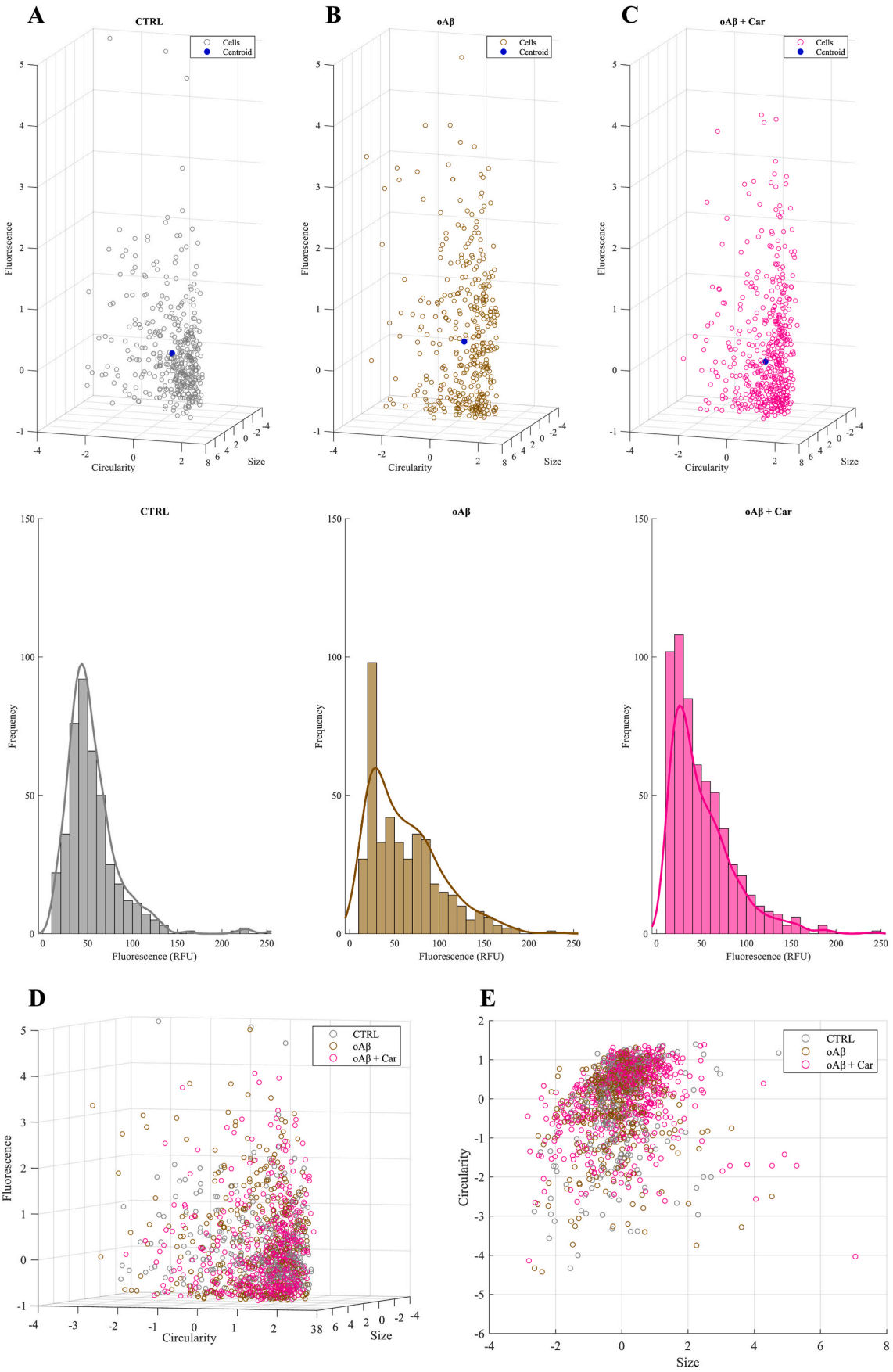

(caption on next page)

Fig. 6. 3D scatterplots and NO fluorescence distributions of mixed glial cells. The 3D scatter plots depict size, circularity, and fluorescence of (A) untreated mixed glial cells, (B) mixed glial cells treated for 24 h with oAβ (2 μM), and (C) mixed glial cells treated for 24 h with oAβ in the presence of carnosine (Car) (10 mM, 1 h pre-treatment). Cytometry data were normalized using the z-score method. No distinguishable clusters were evidenced considering the gap evaluation method for the optimal number of clusters determination. Below each scatterplot is depicted the related fluorescence distribution. Each bin contains the cells in a 10 RFU gap. The overlaid line represents the kernel density estimation of the cells distribution. Fluorescence is expressed as Relative Fluorescence Units (RFU) of DAF-FM. No remarkable differences in distribution of fluorescence are reported. Three samples of each experimental condition were analyzed. Results from the different experimental conditions are individually 3D plotted and merged in (D). 2D scatter considering only size and circularity is shown in (E).

5. Conclusions

In the present study we provided the evidence that carnosine can negatively modulate the oxidative stress induced by oAβ in primary mixed glia cultures by effectively reducing intracellular NO and ROS levels, and mitigating cell-to-cell variability in term of reactive species production. All together our findings open a new path to explore the therapeutic potential of carnosine in oxidative stress driven disorders such as AD.

CRediT authorship contribution statement

Vincenzo Cardaci: Writing – review & editing, Writing – original draft, Validation, Software, Methodology, Investigation, Formal analysis, Data curation. **Lucia Di Pietro:** Writing – review & editing, Software, Methodology, Investigation, Formal analysis, Data curation. **Matthew C. Zupan:** Writing – review & editing, Writing – original draft, Methodology, Investigation, Formal analysis. **Jay Sibbitts:** Writing – review & editing, Methodology, Investigation, Formal analysis, Data curation. **Anna Privitera:** Writing – review & editing, Methodology, Investigation, Formal analysis. **Susan M. Lunte:** Writing – review & editing, Resources, Funding acquisition. **Filippo Caraci:** Writing – review & editing, Resources, Funding acquisition. **Meredith D. Hartley:** Writing – review & editing, Resources, Funding acquisition. **Giuseppe Caruso:** Writing – review & editing, Writing – original draft, Visualization, Validation, Supervision, Resources, Project administration, Funding acquisition, Data curation, Conceptualization.

Funding

GC is a researcher at the University of Catania within the EU-funded PON REACT project (Azione IV.4—"Dottorati e contratti di ricerca su tematiche dell'innovazione", nuovo Asse IV del PON Ricerca e Innovazione 2014–2020 "Istruzione e ricerca per il recupero REACT—EU"; Progetto "Identificazione e validazione di nuovi target farmacologici nella malattia di Alzheimer attraverso l'utilizzo della microfluidica", CUP E65F21002640005). JS is a post-doctoral researcher funded by the National Institutes of Health Institutional Research and Academic Career Development Award (IRACDA) Post-doctoral program hosted by the University of Kansas (#K12GM63651). This research was in part funded by the Italian Ministry of Health Research Program (#RC2022-N4).

MH and MZ were supported by the National Institutes of Health CMADP COBRE (#P20GM103638 and #P30GM145499) and the University of Kansas. MZ received support from the National Institutes of Health Graduate Training at the Biology-Chemistry Interface Grant (#T32 GM132061).

Declaration of interests

The authors declare that they have no known competing financial interests or personal relationships that could have appeared to influence the work reported in this paper.

Acknowledgements

AP would like to thank the International PhD Program in Neuroscience at University of Catania (Italy).

Appendix A. Supplementary data

Supplementary data to this article can be found online at https://doi.org/10.1016/j.freeradbiomed.2025.01.030.

References

[1] A. Kumar, J. Sidhu, F. Lui, J.W. Tsao, Alzheimer disease, in: StatPearls, 2024. Treasure Island (FL).
[2] A.C. Brorsson, J.R. Kumita, I. MacLeod, B. Bolognesi, E. Speretta, L.M. Luheshi, T. P. Knowles, C.M. Dobson, D.C. Crowther, Methods and models in neurodegenerative and systemic protein aggregation diseases, Front. Biosci. 15 (2010) 373–396.
[3] C. Haass, D.J. Selkoe, Soluble protein oligomers in neurodegeneration: lessons from the Alzheimer's amyloid beta-peptide, Nat. Rev. Mol. Cell Biol. 8 (2007) 101–112.
[4] R. Kayed, C.A. Lasagna-Reeves, Molecular mechanisms of amyloid oligomers toxicity, J. Alzheimers Dis. 33 (Suppl 1) (2013) S67–S78.
[5] W.L. Klein, Synaptotoxic amyloid-beta oligomers: a molecular basis for the cause, diagnosis, and treatment of Alzheimer's disease? J. Alzheimers Dis. 33 (Suppl 1) (2013) S49–S65.
[6] W. Wang, F. Zhao, X. Ma, G. Perry, X. Zhu, Mitochondria dysfunction in the pathogenesis of Alzheimer's disease: recent advances, Mol. Neurodegener. 15 (2020) 30.
[7] S. Varadarajan, S. Yatin, M. Aksenova, D.A. Butterfield, Review: alzheimer's amyloid beta-peptide-associated free radical oxidative stress and neurotoxicity, J. Struct. Biol. 130 (2000) 184–208.
[8] D.A. Butterfield, B. Halliwell, Oxidative stress, dysfunctional glucose metabolism and Alzheimer disease, Nat. Rev. Neurosci. 20 (2019) 148–160.
[9] D.A. Butterfield, T. Reed, S.F. Newman, R. Sultana, Roles of amyloid beta-peptide-associated oxidative stress and brain protein modifications in the pathogenesis of Alzheimer's disease and mild cognitive impairment, Free Radic. Biol. Med. 43 (2007) 658–677.
[10] Y. Zhao, B. Zhao, Oxidative stress and the pathogenesis of Alzheimer's disease, Oxid. Med. Cell. Longev. 2013 (2013) 316523.
[11] E. Tamagno, M. Guglielmotto, V. Vasciaveo, M. Tabaton, Oxidative stress and beta amyloid in alzheimer's disease. Which comes first: the chicken or the egg? Antioxidants 10 (2021).
[12] L. Minati, T. Edginton, M.G. Bruzzone, G. Giaccone, Current concepts in Alzheimer's disease: a multidisciplinary review, Am. J. Alzheimers Dis. Other Demen 24 (2009) 95–121.
[13] M. Calvo-Rodriguez, E.K. Kharitonova, A.C. Snyder, S.S. Hou, M.V. Sanchez-Mico, S. Das, Z. Fan, H. Shirani, K.P.R. Nilsson, A. Serrano-Pozo, B.J. Bacskai, Real-time imaging of mitochondrial redox reveals increased mitochondrial oxidative stress associated with amyloid beta aggregates in vivo in a mouse model of Alzheimer's disease, Mol. Neurodegener. 19 (2024) 6.
[14] C. Cheignon, M. Tomas, D. Bonnefont-Rousselot, P. Faller, C. Hureau, F. Collin, Oxidative stress and the amyloid beta peptide in Alzheimer's disease, Redox Biol. 14 (2018) 450–464.
[15] G. Di Benedetto, C. Burgaletto, C.M. Bellanca, A. Munafo, R. Bernardini, G. Cantarella, Role of microglia and astrocytes in alzheimer's disease: from neuroinflammation to Ca(2+) homeostasis dysregulation, Cells 11 (2022).
[16] R.G. Nagele, J. Wegiel, V. Venkataraman, H. Imaki, K.C. Wang, J. Wegiel, Contribution of glial cells to the development of amyloid plaques in Alzheimer's disease, Neurobiol. Aging 25 (2004) 663–674.
[17] L. Katsouri, A.M. Birch, A.W.J. Renziehausen, C. Zach, Y. Aman, H. Steeds, A. Bonsu, E.O.C. Palmer, N. Mirzaei, M. Ries, M. Sastre, Ablation of reactive astrocytes exacerbates disease pathology in a model of Alzheimer's disease, Glia 68 (2020) 1017–1030.
[18] M. Tsacopoulos, P.J. Magistretti, Metabolic coupling between glia and neurons, J. Neurosci. 16 (1996) 877–885.
[19] A. Verkhratsky, M. Nedergaard, Physiology of astroglia, Physiol. Rev. 98 (2018) 239–389.
[20] N. Habib, C. McCabe, S. Medina, M. Varshavsky, D. Kitsberg, R. Dvir-Szternfeld, G. Green, D. Dionne, L. Nguyen, J.L. Marshall, F. Chen, F. Zhang, T. Kaplan, A. Regev, M. Schwartz, Disease-associated astrocytes in Alzheimer's disease and aging, Nat. Neurosci. 23 (2020) 701–706.
[21] C. Escartin, E. Galea, A. Lakatos, J.P. O'Callaghan, G.C. Petzold, A. Serrano-Pozo, C. Steinhauser, A. Volterra, G. Carmignoto, A. Agarwal, N.J. Allen, A. Araque, L. Barbeito, A. Barzilai, D.E. Bergles, G. Bonvento, A.M. Butt, W.T. Chen, M. Cohen-Salmon, C. Cunningham, B. Deneen, B. De Strooper, B. Diaz-Castro, C. Farina, M. Freeman, V. Gallo, J.E. Goldman, S.A. Goldman, M. Gotz, A. Gutierrez, P. G. Haydon, D.H. Heiland, E.M. Hol, M.G. Holt, M. Iino, K.V. Kastanenka, H. Kettenmann, B.S. Khakh, S. Koizumi, C.J. Lee, S.A. Liddelow, B.A. MacVicar, P. Magistretti, A. Messing, A. Mishra, A.V. Molofsky, K.K. Murai, C.M. Norris,

S. Okada, S.H.R. Oliet, J.F. Oliveira, A. Panatier, V. Parpura, M. Pekna, M. Pekny, L. Pellerin, G. Perea, B.G. Perez-Nievas, F.W. Pfrieger, K.E. Poskanzer, F. J. Quintana, R.M. Ransohoff, M. Riquelme-Perez, S. Robel, C.R. Rose, J. D. Rothstein, N. Rouach, D.H. Rowitch, A. Semyanov, S. Sirko, H. Sontheimer, R. A. Swanson, J. Vitorica, I.B. Wanner, L.B. Wood, J. Wu, B. Zheng, E.R. Zimmer, R. Zorec, M.V. Sofroniew, A. Verkhratsky, Reactive astrocyte nomenclature, definitions, and future directions, Nat. Neurosci. 24 (2021) 312–325.

[22] C. Madry, V. Kyrargyri, I.L. Arancibia-Cárcamo, R. Jolivet, S. Kohsaka, R.M. Bryan, D. Attwell, Microglial ramification, surveillance, and interleukin-1β release are regulated by the two-pore domain K(+) channel THIK-1, Neuron 97 (2018) 299–312.e296.

[23] Z. Xie, J. Meng, Z. Wu, H. Nakanishi, Y. Hayashi, W. Kong, F. Lan, Narengaowa, Q. Yang, H. Qing, J. Ni, The dual nature of microglia in alzheimer's disease: a microglia-neuron crosstalk perspective, Neuroscientist 29 (2023) 616–638.

[24] I.P. Karve, J.M. Taylor, P.J. Crack, The contribution of astrocytes and microglia to traumatic brain injury, Br. J. Pharmacol. 173 (2016) 692–702.

[25] C.S. McAlpine, J. Park, A. Griciuc, E. Kim, S.H. Choi, Y. Iwamoto, M.G. Kiss, K. A. Christie, C. Vinegoni, W.C. Poller, J.E. Mindur, C.T. Chan, S. He, H. Janssen, L. P. Wong, J. Downey, S. Singh, A. Anzai, F. Kahles, M. Jorfi, P.F. Feruglio, R. I. Sadreyev, R. Weissleder, B.P. Kleinstiver, M. Nahrendorf, R.E. Tanzi, F. K. Swirski, Astrocytic interleukin-3 programs microglia and limits Alzheimer's disease, Nature 595 (2021) 701–706.

[26] S.A. Liddelow, K.A. Guttenplan, L.E. Clarke, F.C. Bennett, C.J. Bohlen, L. Schirmer, M.L. Bennett, A.E. Munch, W.S. Chung, T.C. Peterson, D.K. Wilton, A. Frouin, B. A. Napier, N. Panicker, M. Kumar, M.S. Buckwalter, D.H. Rowitch, V.L. Dawson, T. M. Dawson, B. Stevens, B.A. Barres, Neurotoxic reactive astrocytes are induced by activated microglia, Nature 541 (2017) 481–487.

[27] M.K. St-Pierre, J. VanderZwaag, S. Loewen, M.E. Tremblay, All roads lead to heterogeneity: the complex involvement of astrocytes and microglia in the pathogenesis of Alzheimer's disease, Front. Cell. Neurosci. 16 (2022) 932572.

[28] C. Schitine, L. Nogaroli, M.R. Costa, C. Hedin-Pereira, Astrocyte heterogeneity in the brain: from development to disease, Front. Cell. Neurosci. 9 (2015) 76.

[29] M.W. Marlatt, J. Bauer, E. Aronica, E.S. van Haastert, J.J. Hoozemans, M. Joels, P. J. Lucassen, Proliferation in the Alzheimer hippocampus is due to microglia, not astroglia, and occurs at sites of amyloid deposition, Neural Plast. 2014 (2014) 693851.

[30] E. Simoncicova, E. Goncalves de Andrade, H.A. Vecchiarelli, I.O. Awogbindin, C. I. Delage, M.E. Tremblay, Present and future of microglial pharmacology, Trends Pharmacol. Sci. 43 (2022) 669–685.

[31] A.A. Boldyrev, G. Aldini, W. Derave, Physiology and pathophysiology of carnosine, Physiol. Rev. 93 (2013) 1803–1845.

[32] J. Spaas, T. Van der Stede, S. de Jager, A. van de Waterweg Berends, A. Tiane, H. Baelde, S.P. Baba, M. Eckhardt, E. Wolfs, T. Vanmierlo, N. Hellings, B.O. Eijnde, W. Derave, Carnosine synthase deficiency aggravates neuroinflammation in multiple sclerosis, Prog. Neurobiol. 231 (2023) 102532.

[33] B. Herculano, M. Tamura, A. Ohba, M. Shimatani, N. Kutsuna, T. Hisatsune, beta-alanyl-L-histidine rescues cognitive deficits caused by feeding a high fat diet in a transgenic mouse model of Alzheimer's disease, J. Alzheimers Dis. 33 (2013) 983–997.

[34] S. Fleisher-Berkovich, C. Abramovitch-Dahan, S. Ben-Shabat, R. Apte, E. Beit-Yannai, Inhibitory effect of carnosine and N-acetyl carnosine on LPS-induced microglial oxidative stress and inflammation, Peptides 30 (2009) 1306–1312.

[35] L. Ou-Yang, Y. Liu, B.Y. Wang, P. Cao, J.J. Zhang, Y.Y. Huang, Y. Shen, J.X. Lyu, Carnosine suppresses oxygen-glucose deprivation/recovery-induced proliferation and migration of reactive astrocytes of rats in vitro, Acta Pharmacol. Sin. 39 (2018) 24–34.

[36] G. Caruso, C.G. Fresta, N. Musso, M. Giambirtone, M. Grasso, S.F. Spampinato, S. Merlo, F. Drago, G. Lazzarino, M.A. Sortino, S.M. Lunte, F. Caraci, Carnosine prevents abeta-induced oxidative stress and inflammation in microglial cells: a key role of TGF-beta1, Cells 8 (2019).

[37] G. Caruso, C. Benatti, N. Musso, C.G. Fresta, A. Fidilio, G. Spampinato, N. Brunello, C. Bucolo, F. Drago, S.M. Lunte, B.R. Peterson, F. Tascedda, F. Caraci, Carnosine protects macrophages against the toxicity of aβ1-42 oligomers by decreasing oxidative stress, Biomedicines 9 (2021).

[38] G. Caruso, C.G. Fresta, F. Martinez-Becerra, L. Antonio, R.T. Johnson, R.P.S. de Campos, J.M. Siegel, M.B. Wijesinghe, G. Lazzarino, S.M. Lunte, Carnosine modulates nitric oxide in stimulated murine RAW 264.7 macrophages, Mol. Cell. Biochem. 431 (2017) 197–210.

[39] C.G. Fresta, A. Chakraborty, M.B. Wijesinghe, A.M. Amorini, G. Lazzarino, G. Lazzarino, B. Tavazzi, S.M. Lunte, F. Caraci, P. Dhar, G. Caruso, Non-toxic engineered carbon nanodiamond concentrations induce oxidative/nitrosative stress, imbalance of energy metabolism, and mitochondrial dysfunction in microglial and alveolar basal epithelial cells, Cell Death Dis. 9 (2018) 245.

[40] C.G. Fresta, A. Fidilio, G. Lazzarino, N. Musso, M. Grasso, S. Merlo, A.M. Amorini, C. Bucolo, B. Tavazzi, G. Lazzarino, S.M. Lunte, F. Caraci, G. Caruso, Modulation of pro-oxidant and pro-inflammatory activities of M1 macrophages by the natural dipeptide carnosine, Int. J. Mol. Sci. 21 (2020).

[41] F. Caraci, F. Tascedda, S. Merlo, C. Benatti, S.F. Spampinato, A. Munafo, G. M. Leggio, F. Nicoletti, N. Brunello, F. Drago, M.A. Sortino, A. Copani, Fluoxetine prevents abeta(1-42)-induced toxicity via a paracrine signaling mediated by transforming-growth-factor-beta1, Front. Pharmacol. 7 (2016) 389.

[42] A. Distefano, G. Caruso, V. Oliveri, F. Bellia, D. Sbardella, G.A. Zingale, F. Caraci, G. Grasso, Neuroprotective effect of carnosine is mediated by insulin-degrading enzyme, ACS Chem. Neurosci. 13 (2022) 1588–1593.

[43] H. Lian, E. Roy, H. Zheng, Protocol for primary microglial culture preparation, Bio-protocol 6 (2016) e1989.

[44] C.G. Fresta, M.L. Hogard, G. Caruso, E.E. Melo Costa, G. Lazzarino, S.M. Lunte, Monitoring carnosine uptake by RAW 264.7 macrophage cells using microchip electrophoresis with fluorescence detection, Anal. Methods 9 (2017) 402–408.

[45] G. Caruso, C.G. Fresta, A. Fidilio, F. Lazzara, N. Musso, V. Cardaci, F. Drago, F. Caraci, C. Bucolo, Carnosine counteracts the molecular alterations aβ oligomers-induced in human retinal pigment epithelial cells, Molecules 28 (2023).

[46] J. Sibbitts, C.T. Culbertson, Measuring stimulation and inhibition of intracellular nitric oxide production in SIM-A9 microglia using microfluidic single-cell analysis, Anal. Methods 12 (2020) 4665–4673.

[47] E.R. Mainz, D.B. Gunasekara, G. Caruso, D.T. Jensen, M.K. Hulvey, J.A.F. Da Silva, E.C. Metto, A.H. Culbertson, C.T. Culbertson, S.M. Lunte, Monitoring intracellular nitric oxide production using microchip electrophoresis and laser-induced fluorescence detection, Anal. Methods 4 (2012) 414–420.

[48] G. Caruso, C.G. Fresta, A. Fidilio, F. O'Donnell, N. Musso, G. Lazzarino, M. Grasso, A.M. Amorini, F. Tascedda, C. Bucolo, F. Drago, B. Tavazzi, G. Lazzarino, S. M. Lunte, F. Caraci, Carnosine decreases PMA-induced oxidative stress and inflammation in murine macrophages, Antioxidants 8 (2019).

[49] R.P. de Campos, J.M. Siegel, C.G. Fresta, G. Caruso, J.A. da Silva, S.M. Lunte, Indirect detection of superoxide in RAW 264.7 macrophage cells using microchip electrophoresis coupled to laser-induced fluorescence, Anal. Bioanal. Chem. 407 (2015) 7003–7012.

[50] D. Bongiorno, N. Musso, G. Caruso, L.M. Lazzaro, F. Caraci, S. Stefani, F. Campanile, Staphylococcus aureus ST228 and ST239 as models for expression studies of diverse markers during osteoblast infection and persistence, Microbiol. 10 (2021) e1178.

[51] J. Cáceres-Del-Carpio, M.T. Moustafa, J. Toledo-Corral, M.A. Hamid, S.R. Atilano, K. Schneider, P.S. Fukuhara, R.D. Costa, J.L. Norman, D. Malik, M. Chwa, D. S. Boyer, G.A. Limb, M.C. Kenney, B.D. Kuppermann, In vitro response and gene expression of human retinal Müller cells treated with different anti-VEGF drugs, Exp. Eye Res. 191 (2020) 107903.

[52] A.R. Hipkiss, J.E. Preston, D.T. Himsworth, V.C. Worthington, M. Keown, J. Michaelis, J. Lawrence, A. Mateen, L. Allende, P.A. Eagles, N.J. Abbott, Pluripotent protective effects of carnosine, a naturally occurring dipeptide, Ann. N. Y. Acad. Sci. 854 (1998) 37–53.

[53] G. Caruso, L. Di Pietro, V. Cardaci, S. Maugeri, F. Caraci, The therapeutic potential of carnosine: focus on cellular and molecular mechanisms, Curr. Res. Pharmacol Drug Discov. 4 (2023) 100153.

[54] V.D. Prokopieva, E.G. Yarygina, N.A. Bokhan, S.A. Ivanova, Use of carnosine for oxidative stress reduction in different pathologies, Oxid. Med. Cell. Longev. 2016 (2016) 2939087.

[55] F. Attanasio, M. Convertino, A. Magno, A. Caflisch, A. Corazza, H. Haridas, G. Esposito, S. Cataldo, B. Pignataro, D. Milardi, E. Rizzarelli, Carnosine inhibits Aβ (42) aggregation by perturbing the H-bond network in and around the central hydrophobic cluster, Chembiochem 14 (2013) 583–592.

[56] A. Aloisi, A. Barca, A. Romano, S. Guerrieri, C. Storelli, R. Rinaldi, T. Verri, Anti-aggregating effect of the naturally occurring dipeptide carnosine on aβ1-42 fibril formation, PLoS One 8 (2013) e68159.

[57] M. Kubota, N. Kobayashi, T. Sugizaki, M. Shimoda, M. Kawahara, K.-i. Tanaka, Carnosine suppresses neuronal cell death and inflammation induced by 6-hydroxydopamine in an in vitro model of Parkinson's disease, PLoS One 15 (2020) e0240448.

[58] G. Caruso, F. Caraci, R.B. Jolivet, Pivotal role of carnosine in the modulation of brain cells activity: multimodal mechanism of action and therapeutic potential in neurodegenerative disorders, Prog. Neurobiol. 175 (2019) 35–53.

[59] A.N. Fonteh, R.J. Harrington, A. Tsai, P. Liao, M.G. Harrington, Free amino acid and dipeptide changes in the body fluids from Alzheimer's disease subjects, Amino Acids 32 (2007) 213–224.

[60] M.P. Mattson, Pathways towards and away from Alzheimer's disease, Nature 430 (2004) 631–639.

[61] D.A. Butterfield, A.M. Swomley, R. Sultana, Amyloid beta-peptide (1-42)-induced oxidative stress in Alzheimer disease: importance in disease pathogenesis and progression, Antioxidants Redox Signal. 19 (2013) 823–835.

[62] G. Karapetyan, K. Fereshetyan, H. Harutyunyan, K. Yenkoyan, The synergy of beta amyloid 1-42 and oxidative stress in the development of Alzheimer's disease-like neurodegeneration of hippocampal cells, Sci. Rep. 12 (2022) 17883.

[63] R.G. Roy, P.K. Mandal, J.C. Maroon, Oxidative stress occurs prior to amyloid abeta plaque formation and tau phosphorylation in alzheimer's disease: role of glutathione and metal ions, ACS Chem. Neurosci. 14 (2023) 2944–2954.

[64] A. Houldsworth, Role of oxidative stress in neurodegenerative disorders: a review of reactive oxygen species and prevention by antioxidants, Brain Commun. 6 (2024) fcad356.

[65] E.O. Olufunmilayo, M.B. Gerke-Duncan, R.M.D. Holsinger, Oxidative stress and antioxidants in neurodegenerative disorders, Antioxidants 12 (2023).

[66] M. Ghasemi, T. Turnbull, S. Sebastian, I. Kempson, The MTT assay: utility, limitations, pitfalls, and interpretation in bulk and single-cell analysis, Int. J. Mol. Sci. 22 (2021).

[67] S. Söllvander, E. Nikitidou, R. Brolin, L. Söderberg, D. Sehlin, L. Lannfelt, A. Erlandsson, Accumulation of amyloid-β by astrocytes result in enlarged endosomes and microvesicle-induced apoptosis of neurons, Mol. Neurodegener. 11 (2016) 38.

[68] P. Kerokoski, H. Soininen, T. Pirttilä, Beta-amyloid (1-42) affects MTT reduction in astrocytes: implications for vesicular trafficking and cell functionality, Neurochem. Int. 38 (2001) 127–134.

[69] B.R. Mun, S.B. Park, W.S. Choi, The oligomeric form of amyloid beta triggers astrocyte activation, independent of neurons, Chonnam Med. J. 60 (2024) 27–31.

[70] C.J. Garwood, A.M. Pooler, J. Atherton, D.P. Hanger, W. Noble, Astrocytes are important mediators of Aβ-induced neurotoxicity and tau phosphorylation in primary culture, Cell Death Dis. 2 (2011) e167.
[71] R.G. Nagele, M.R. D'Andrea, H. Lee, V. Venkataraman, H.Y. Wang, Astrocytes accumulate A beta 42 and give rise to astrocytic amyloid plaques in Alzheimer disease brains, Brain Res. 971 (2003) 197–209.
[72] H.M. Nielsen, S.D. Mulder, J.A. Beliën, R.J. Musters, P. Eikelenboom, R. Veerhuis, Astrocytic A beta 1-42 uptake is determined by A beta-aggregation state and the presence of amyloid-associated proteins, Glia 58 (2010) 1235–1246.
[73] T. Togo, O. Katsuse, E. Iseki, Nitric oxide pathways in Alzheimer's disease and other neurodegenerative dementias, Neurol. Res. 26 (2004) 563–566.
[74] C.A. Massaad, R.G. Pautler, E. Klann, Mitochondrial superoxide: a key player in Alzheimer's disease, Aging (Albany NY) 1 (2009) 758–761.
[75] C. Corona, V. Frazzini, E. Silvestri, R. Lattanzio, R. La Sorda, M. Piantelli, L. M. Canzoniero, D. Ciavardelli, E. Rizzarelli, S.L. Sensi, Effects of dietary supplementation of carnosine on mitochondrial dysfunction, amyloid pathology, and cognitive deficits in 3xTg-AD mice, PLoS One 6 (2011) e17971.
[76] G. Caruso, A. Privitera, M.W. Saab, N. Musso, S. Maugeri, A. Fidilio, A.P. Privitera, A. Pittalà, R.B. Jolivet, L. Lanzanò, G. Lazzarino, F. Caraci, A.M. Amorini, Characterization of carnosine effect on human microglial cells under basal conditions, Biomedicines 11 (2023).
[77] A. Privitera, V. Cardaci, D. Weerasekara, M.W. Saab, L. Diolosà, A. Fidilio, R. B. Jolivet, G. Lazzarino, A.M. Amorini, M. Camarda, S.M. Lunte, F. Caraci, G. Caruso, Microfluidic/HPLC combination to study carnosine protective activity on challenged human microglia: focus on oxidative stress and energy metabolism, Front. Pharmacol. 14 (2023) 1161794.
[78] G.I. Klebanov, O. Teselkin Yu, I.V. Babenkova, I.N. Popov, G. Levin, O.V. Tyulina, A.A. Boldyrev, A. Vladimirov Yu, Evidence for a direct interaction of superoxide anion radical with carnosine, Biochem. Mol. Biol. Int. 43 (1997) 99–106.
[79] J. Spaas, W.M.A. Franssen, C. Keytsman, L. Blancquaert, T. Vanmierlo, J. Bogie, B. Broux, N. Hellings, J. van Horssen, D.K. Posa, D. Hoetker, S.P. Baba, W. Derave, B.O. Eijnde, Carnosine quenches the reactive carbonyl acrolein in the central nervous system and attenuates autoimmune neuroinflammation, J. Neuroinflammation 18 (2021) 255.
[80] K. Kulebyakin, L. Karpova, E. Lakonsteva, M. Krasavin, A. Boldyrev, Carnosine protects neurons against oxidative stress and modulates the time profile of MAPK cascade signaling, Amino Acids 43 (2012) 91–96.
[81] A.V. Lopachev, O.M. Lopacheva, D.A. Abaimov, O.V. Koroleva, E. A. Vladychenskaya, A.A. Erukhimovich, T.N. Fedorova, Neuroprotective effect of carnosine on primary culture of rat cerebellar cells under oxidative stress, Biochemistry (Mosc.) 81 (2016) 511–520.
[82] F. Attanasio, S. Cataldo, S. Fisichella, S. Nicoletti, V.G. Nicoletti, B. Pignataro, A. Savarino, E. Rizzarelli, Protective effects of L- and D-carnosine on alpha-crystallin amyloid fibril formation: implications for cataract disease, Biochemistry 48 (2009) 6522–6531.
[83] S. Javadi, R. Yousefi, S. Hosseinkhani, A.M. Tamaddon, V.N. Uversky, Protective effects of carnosine on dehydroascorbate-induced structural alteration and opacity of lens crystallins: important implications of carnosine pleiotropic functions to combat cataractogenesis, J. Biomol. Struct. Dyn. 35 (2017) 1766–1784.
[84] S.K. Bardaweel, M. Gul, M. Alzweiri, A. Ishaqat, A.L. Ha, R.M. Bashatwah, Reactive oxygen species: the dual role in physiological and pathological conditions of the human body, Eurasian J. Med. 50 (2018) 193–201.
[85] F.X. Guix, I. Uribesalgo, M. Coma, F.J. Muñoz, The physiology and pathophysiology of nitric oxide in the brain, Prog. Neurobiol. 76 (2005) 126–152.
[86] P. Preman, M. Alfonso-Triguero, E. Alberdi, A. Verkhratsky, A.M. Arranz, Astrocytes in alzheimer's disease: pathological significance and molecular pathways, Cells 10 (2021).
[87] H.Z. Long, Z.W. Zhou, Y. Cheng, H.Y. Luo, F.J. Li, S.G. Xu, L.C. Gao, The role of microglia in alzheimer's disease from the perspective of immune inflammation and iron metabolism, Front. Aging Neurosci. 14 (2022) 888989.
[88] W. Qu, P. Canoll, G. Hargus, Molecular insights into cell type-specific roles in alzheimer's disease: human induced pluripotent stem cell-based disease modelling, Neuroscience 518 (2023) 10–26.
[89] R. Liu, X. Meng, X. Yu, G. Wang, Z. Dong, Z. Zhou, M. Qi, X. Yu, T. Ji, F. Wang, From 2D to 3D Co-culture systems: a review of Co-culture models to study the neural cells interaction, Int. J. Mol. Sci. 23 (2022).
[90] Y. Wu, U.L.M. Eisel, Microglia-astrocyte communication in alzheimer's disease, J. Alzheimers Dis. 95 (2023) 785–803.
[91] D. Singh, Astrocytic and microglial cells as the modulators of neuroinflammation in Alzheimer's disease, J. Neuroinflammation 19 (2022) 206.